NASA-CR-193030

THE BRADLEY DEPARTMENT OF ELECTRICAL ENGINEERING

VIRGINIA TECH

SEMIANNUAL STATUS REPORT FOR

"FEASIBILITY STUDY OF A SYNTHESIS PROCEDURE FOR ARRAY FEEDS TO IMPROVE RADIATION PERFORMANCE OF LARGE DISTORTED REFLECTOR ANTENNAS"

by

W.L. Stutzman, K. Takamizawa, P. Werntz,
J. LaPean, B. Shen

March 1993

SATCOM Report No. 93-3

VIRGINIA TECH
Satellite Communications Group

VIRGINIA POLYTECHNIC INSTITUTE AND STATE UNIVERSITY
Blacksburg, Virginia 24061 (703)231-6646

FEASIBILITY STUDY OF A SYNTHESIS PROCEDURE FOR ARRAY FEEDS TO IMPROVE RADIATION PERFORMANCE OF LARGE DISTORTED REFLECTOR ANTENNAS

SEMIANNUAL STATUS REPORT

submitted to
NASA Langley Research Center
for
Grant No. NAG-1-859

by

W.L. Stutzman
K. Takamizawa
P. Werntz
J. LaPean
B. Shen

Virginia Polytechnic Institute and State University
Bradley Department of Electrical Engineering
Blacksburg, Virginia 24061-0111

SATCOM Report No. 93-3

March 1993

semiann1
04/27/93

TABLE OF CONTENTS

I. INTRODUCTION

1.1 Project Organization

Virginia Tech has several activities which support the NASA Langley effort in the area of large aperture radiometric antenna systems. These activities are summarized in Table 1-1. This semi-annual report reports on these activities. Table 1-2 lists major reflector antenna research areas at Virginia Tech together with the graduate students responsible for the work.

Table 1-1

Personnel at Virginia Tech Performing Reflector Antenna Research

Reflector Antenna Research at Virginia Tech

1. "Feasibility Study of a Synthesis Procedure for Array Feeds to Improve Radiation Performance of Large Distorted Reflector Antennas"
   GAs: Ko Takamizawa, B. Shen
   Project: NASA Grant NAG-1-859; VT 4-26132
   Term: 02/25/88 - 12/31/93

Personnel Active in Reflectors but not Supported by NASA

2. R. Michael Barts
   "Design of Array Feeds for Large Reflector Antennas," NASA Graduate Researchers Program Grant NGT-50413; completed, but work continues.

3. Derrick Dunn, M.S. student
   Support: GEM Fellowship (6/91 to 12/92); NASA Traineeship (1/93 -)

4. Jim LaPean

5. Paul Werntz

6. Marco Terada

Table 1-2

Reflector Antenna Research Activities at Virginia Tech

I. Technology Development

1.1. Operation and testing of full commercial reflector code (GRASP7) - Takamizawa

1.2. Documentation of analysis techniques for reflector computations - Takamizawa

1.3. Beam efficiency studies - Shen

II. Wide Scanning Antenna Systems

2.1. Documentation of wide scanning antenna principles - Werntz

2.2. Type 1 dual-reflector design - LaPean

2.3. Type 2 tri-reflector antenna design - Werntz

2.4. Support of Type 1 and 2 hardware model - LaPean and Werntz

2.5. Spherical reflector antenna designs - Shen

III. Reflector System Optimization - Takamizawa

3.1. Comparison of optimization techniques

3.2. Error functional definition

IV. Arrays for Large Radiometric Antennas - Barts

4.1. Analysis techniques in lossy radiometric systems using arrays.

4.2. Feed array architectures for radiometers

4.3. Feed component technology readiness evaluation

4.4. Calibration issues

1.2 Overview of Semi-Annual Progress

Significant progress has occurred in this past six-month reporting period. This largely occurred due to previous ground work laid by graduate students and now these efforts are coming to fruition. The Type 1 antenna is complete and documentation is in final phases. The Type 2 antenna design is complete; a journal article has been submitted. The spherical antenna configurations are complete and a journal article will appear in IEEE Transactions on Antennas and Propagation. In addition, a patent for the spherical antenna is being pursued. The final current activity is that of optimization techniques and they are approaching completion as well. All of the four foregoing activities will result in a thesis/dissertation. Copies will be provided to NASA. Also, manuscripts for journal articles will be prepared and submitted to NASA for approval. See Chapter 4 for a summary of publications.

Another recent activity worthy of note is computer code development and integration. Figure 1-1 provides an overview of the computer codes in use at Virginia Tech in support of reflector antenna design.

The heart of this code is GRASP7. This code, originally intended for mainframe use, has been operated on high-end PCs at Virginia Tech for two years. Recently, we have written and implemented pre and post processing code modules. EASY7 is a user friendly code used to create an input file to GRASP7. UVPLOT and UVSTAT are codes which create output information files. The commercial plotting code AXUM is then used to generate pattern plots on a laser printer.

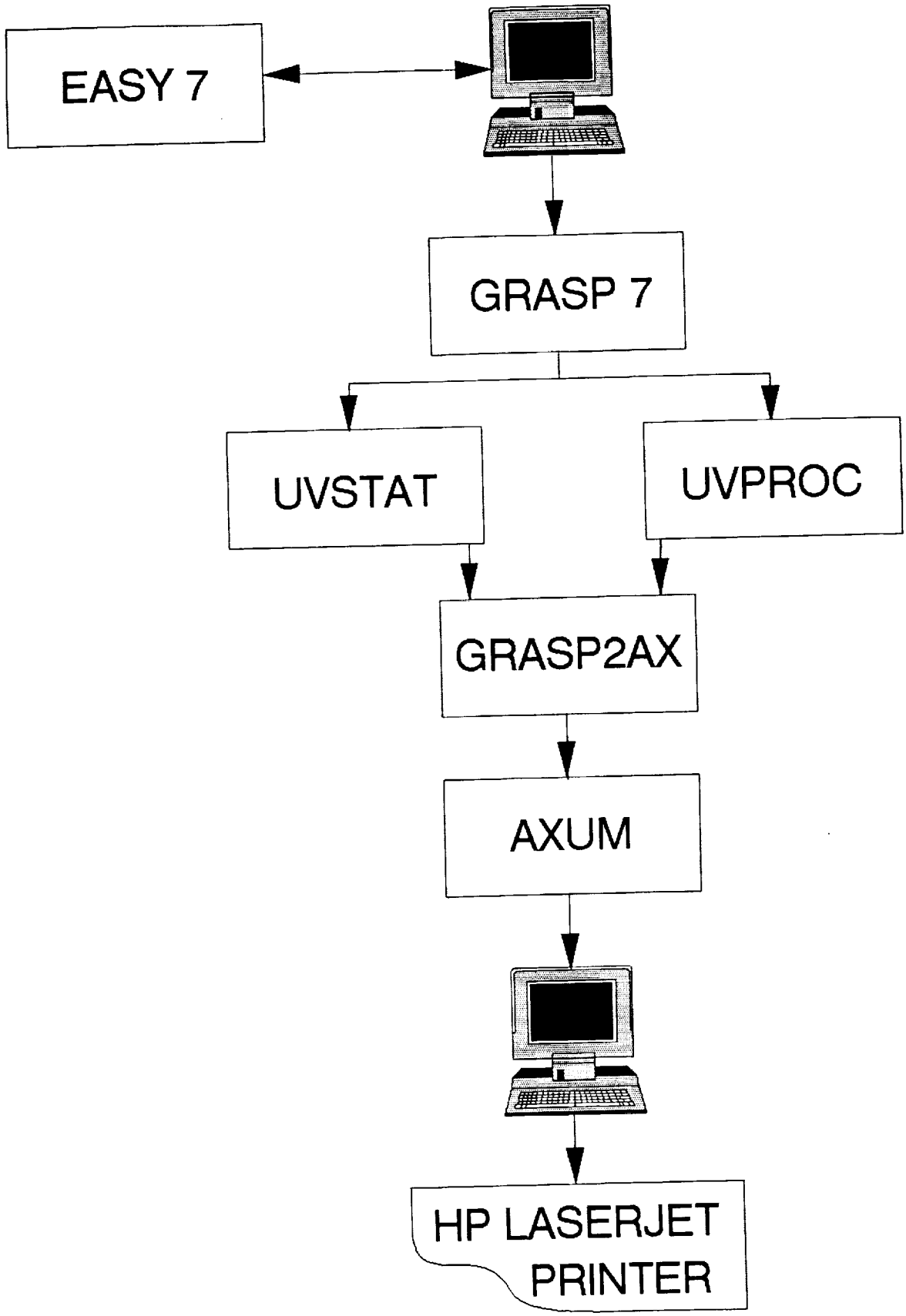

Figure 1-1. Block diagram of reflector antenna codes.

Chapter 2
THE IMPROVED SPHERICAL TRI-REFLECTOR SYSTEM WITH A FLAT MIRROR

The low aperture efficiency problem common in spherical tri-reflector systems was overcome by the tri-reflector design as described in the previous semi-annual report. This tri-reflector design employs a suboptics assembly that consists of two subreflectors and a feed, which are moved as a unit during scan. In order to further simplify the mechanical motion, and therefore, improve practicality of such systems, studies were performed on techniques to reduce the mechanical complexity of motion. In a typical configuration, the moving subreflector and tertiary should be as small as possible and the feed should remain fixed. Watanabe et al. [16] proposed a beam waveguide configuration which permits a fixed feed. The beam waveguide portion consists of two prime focus parabolic reflectors, and creates the image of the real feed. The beam waveguide moves in such a way that the image of the real feed moves as required for scan. This, of course, reduces the complexity of the feed; however, the massive beam waveguide must move in addition to the subreflector and tertiary.

In order to reduce the mass of moving parts in the antenna system, we investigated various optical configurations which form movable images of the suboptics assembly. We found that with proper placement of a planar mirror, an image of the entire suboptics assembly is created without blockage. Scan can then be achieved by rotating the mirror, creating a rotating image of the suboptics assembly. The system designed for the test case (Bush model) scans $\pm 5^{\circ}$ in both orthogonal directions. Since the mirror creates the image of the entire suboptics assembly, not only is the feed fixed, but the subreflector and the tertiary are all fixed.

2.1. Fixing the Suboptics Assembly by Mirror Imaging

The configuration that permits the suboptics assembly to remained fixed uses a mirror as illustrated in Fig. 2-1, which shows a dual-caustic spherical tri-reflector system [1] in Fig. 2-1a and the version with a mirror in Fig. 2-1b. The mirror creates the image of the suboptics assembly as shown in Fig. 2-1c, and behaves effectively the same during scan as the real suboptics assembly in Fig. 2-1a. This is because, according to geometrical optics (GO) principles, a mirror creates an image without aberration. Physical optics (PO) shows that diffraction loss is present because of the finite size of the mirror. However, in the designs we have encountered, diffraction loss is negligible.

The suboptics in Fig. 2-1 is synthesized by our PDE method, which solves a set of partial differential equations to generate the surface shapes of dual subreflectors. The

dual-subreflector system controls both aperture phase and amplitude. The suboptics assembly in Fig. 2-1a is placed in such a way that the output main beam is parallel to z axis, which is the *antenna coordinate*. In Fig. 2-1b the real suboptics assembly is identical to that in Fig. 2-1a. The plane containing the mirror in Fig. 2-1b passes though the center, O, of the spherical main reflector. Thus, the image of the suboptics assembly in Fig. 2-1c creates an output main beam that is parallel to z′ axis and forms an angle θ from z axis. Scan is achieved by rotating the mirror about O, and therefore, rotating the virtual suboptics and the main beam. The main beam can be directed anywhere inside a spherical cone angle of $\theta_s = 5^\circ$ relative to the unscanned beam direction (z_s - axis, which is offset $\theta = 10^\circ$ from the z-axis). This is accomplished through control of two rotation angles of the mirror about the spherical center point, 0, which we now describe.

One mirror rotation angle (α) is the angle between the mirror plane and z axis, and the other angle (ϕ) is the azimuthal angle of the mirror surface normal; see Fig. 2-2 for the geometry. The mirror creates the image of the z axis; this virtual axis is called z′ and is parallel to the output main beam from the spherical main reflector. Therefore, the angle θ between the virtual axis (z′) and the z axis (θ-scan angle) is 2α. On the other hand, it is obvious to from Fig. 2-2 that the azimuthal angle of the mirror surface normal ($\hat{n}$) is the same azimuthal angle as for the virtual z′ axis (ϕ-scan angle). These geometrical relationships are summarized as follows:

$$\begin{cases} 2\,\alpha_{\text{mirror}} = \theta \\ \\ \phi_{\text{mirror}} = \phi \end{cases} \tag{2-1}$$

These results specify the mechanical rotation of the mirror required for scan of the main output beam.

2.2. Improving the Aperture Efficiency by Tilting the Feed in Azimuth

The movement of the mirror described in the last section scans the main beam; however, it also introduces movement of the main reflector illuminated area, assuming the feed remains fixed during scan. This, of course, reduces the aperture efficiency. In fact, the motion of the main reflector illuminated area can be so severe (especially during ϕ-scan) that the aperture utilization becomes unacceptable (<30%) for $\pm 5^\circ$ circular scan coverage.

The problem of poor aperture utilization can be greatly alleviated by implementing the feed tilt method. By tilting the feed in both azimuth and elevation, the main reflector illuminated area can be totally fixed during scan, and therefore, the aperture

efficiency can be as high as 70% (see the next chapter). In practice, it is much easier to tilt the feed only in azimuth (that is, the feed rotates as angle ϕ in the xy-plane; see Fig. 2-2) than in both angles. Azimuth feed tilt greatly reduces the motion of the aperture illuminated area, although it allows the aperture illumination to move during θ-scan. The aperture efficiency for azimuth only feed tilt (about 50%; see the next chapter) is less than the 70% aperture efficiency obtained when the feed is tilted in both azimuth and elevation; however, it is a great improvement from the fixed feed case. For most practical applications, the azimuth-only feed tilt method is the most advantageous considering the trade-off between aperture efficiency and feed system complicity.

Detailed aperture utilization analysis is necessary to show the effectiveness of feed tilting method and to obtain the proper feed tilting angle as a function of scan angle. The key to the aperture utilization analysis is to study the motion of the center of the aperture illuminated area, which is marked C′ in Fig. 2-2. The mirror image of C′ is C, which is the center of "illumination" for the virtual main reflector. C does not move when the mirror is rotated to scan, it only moves when the feed tilts. C′ is the mirror image of C, and is found by (2-2)

$$\vec{r}'_c = \vec{r}_c - 2\,(\hat{n}\cdot\vec{r}_c)\,\hat{n} \tag{2-2}$$

where $\hat{n}$ is the surface normal of the mirror. A mirror coordinate system is established with x_m axis along $\hat{n}$, and y_m axis in the plane of x and y; see Fig. 2-2. The coordinate transformation between the antenna coordinates (x, y, z) and the mirror coordinates can be written as

$$\begin{bmatrix} x \\ y \\ z \end{bmatrix} = \begin{bmatrix} \cos\alpha\cos\phi & -\sin\phi & \sin\alpha\cos\phi \\ \cos\alpha\sin\phi & \cos\phi & \sin\alpha\sin\phi \\ -\sin\alpha & & \cos\alpha \end{bmatrix} \begin{bmatrix} x' \\ y' \\ z' \end{bmatrix} = \mathrm{T} \begin{bmatrix} x' \\ y' \\ z' \end{bmatrix} \tag{2-3}$$

This coordinate rotation matrix, T, with $\hat{n}=\hat{x}_m$ permits (2-2) to be written as (in the antenna coordinates)

$$\begin{bmatrix} x'_c \\ y'_c \\ z'_c \end{bmatrix} = \mathrm{T} \begin{bmatrix} -1 & 0 & 0 \\ 0 & 1 & 0 \\ 0 & 0 & 1 \end{bmatrix} \mathrm{T}^t \begin{bmatrix} x_c \\ y_c \\ z_c \end{bmatrix} = \mathrm{R} \begin{bmatrix} x_c \\ y_c \\ z_c \end{bmatrix} \tag{2-4}$$

where T^t is the transpose of T. The general mirror reflection matrix, which gives the mirror image of any vector, is formed by multiplying out the three matrices in (2-4) giving

$$R = \begin{bmatrix} -\cos\theta\cos^2\phi+\sin^2\phi & -(\cos\theta+1)\frac{\sin2\phi}{2} & \sin\theta\cos\phi \\ -(\cos\theta+1)\frac{\sin2\phi}{2} & -\cos\theta\sin^2\phi+\cos^2\phi & \sin\theta\sin\phi \\ \sin\theta\cos\phi & \sin\theta\sin\phi & 1 \end{bmatrix} \qquad (2\text{-}5)$$

where θ and ϕ are scan angles in antenna coordinates and (2-1) is used to replace α with θ.

For simplicity, we first consider a fixed feed which causes the "illumination" center of the virtual main reflector, C, to lie in the xz-plane (ϕ_c=0); the direction to C, $\vec{r}_c$, forms angle θ_c from the $-z$ axis. Therefore, point C′ on the sphere is expressed in antenna coordinates as

$$\hat{r}'_c = R\,\vec{r}_c = \begin{bmatrix} (\cos\theta\cos^2\phi-\sin^2\phi)\sin\theta_c-\sin\theta\cos\phi\cos\theta_c \\ (\cos\theta+1)\frac{\sin2\phi}{2}\sin\theta_c-\sin\theta\sin\phi\cos\theta_c \\ -\sin\theta\cos\phi\sin\theta_c-\cos\theta_c \end{bmatrix} \qquad (2\text{-}6)$$

where the angle between $\hat{r}'_c$ and $-z$ axis is θ'_c, and the azimuth angle of $\hat{r}'_c$ in the xy plane is ϕ'_c; they are found by coordinates of $\hat{r}'_c$ in (2-6) as

$$\tan\theta'_c = -\frac{x'_c}{z'_c} = \frac{(\cos\theta\cos^2\phi-\sin^2\phi)\sin\theta_c-\sin\theta\cos\phi\cos\theta_c}{\sin\theta\cos\phi\sin\theta_c+\cos\theta_c} \qquad (2\text{-}7)$$

and,

$$\tan\phi'_c = \frac{x'_c}{y'_c} = \frac{(\cos\theta+1)\frac{\sin2\phi}{2}\sin\theta_c-\sin\theta\sin\phi\cos\theta_c}{(\cos\theta\cos^2\phi-\sin^2\phi)\sin\theta_c-\sin\theta\cos\phi\cos\theta_c} \qquad (2\text{-}8)$$

The functional relationship between ϕ'_c and ϕ given in (2-8) is of particular interest, and is plotted as the $\phi_c = 0^\circ$ curve in Fig. 2-3 (0° feed tilt). This curve shows that the change of ϕ'_c is more than double the change of ϕ. This means that the azimuth angle of the main reflector illumination center C′ is very sensitive to ϕ scan, due to mirror rotation during ϕ-scan. Furthermore, as explained in the following discussion, a large dynamic ϕ-scan range is required to cover a normal circular scan region; e.g. $\pm 5^\circ$ scan requires $\pm 28^\circ$ ϕ-scan range.

The large ϕ-scan range requirement is a disadvantage of this system. This requirement is explained through Fig. 2-4. The z_s axis in Fig. 2-4 is directed toward the center of the scan region and forms angle θ_0 from the z axis. The angle θ_0 is non zero because of the offsetting for the antenna system. (This is illustrated in Fig. 2-1b, where the main output beam cannot be parallel to the z-axis.) However, the offsetting only occurs in the xz plane. We establish a scan coordinate system with x_s axis in the xy

plane and y_s axis the same as y axis. The coordinate transformation between scan coordinates and antenna coordinates is

$$\begin{bmatrix} x \\ y \\ z \end{bmatrix} = \begin{bmatrix} \cos\theta_0 & & \sin\theta_0 \\ & 1 & \\ -\sin\theta_0 & & \cos\theta_0 \end{bmatrix} \begin{bmatrix} x_s \\ y_s \\ z_s \end{bmatrix} \tag{2-9}$$

For a main beam direction (z′ direction) with scan angles θ_s from z_s axis and azimuthal angle ϕ_s in the scan coordinates, the (θ, ϕ) angles in the antenna coordinates can be found from (2-9) as

$$\begin{bmatrix} \sin\theta\cos\phi \\ \sin\theta\sin\phi \\ \cos\theta \end{bmatrix} = \begin{bmatrix} \cos\theta_0 \sin\theta_s \cos\phi_s + \sin\theta_0 \cos\theta_s \\ \sin\theta_s \sin\phi_s \\ -\sin\theta_0 \sin\theta_s \cos\phi_s + \cos\theta_0 \cos\theta_s \end{bmatrix} \tag{2-10}$$

The azimuthal angle ϕ in antenna coordinates is, therefore,

$$\tan\phi = \frac{\sin\theta_s \sin\phi_s}{\cos\theta_0 \sin\theta_s \cos\phi_s + \sin\theta_0 \cos\theta_s} \tag{2-11}$$

Since we are interested in the maximum (mirror rotation) ϕ angle required to perform scan, the change of ϕ along the boundary of the scan region is of particular interest. This boundary for our test case is θ_s=5° and ϕ_s=0° ~ 360°. The corresponding values of ϕ as a function of ϕ_s along the boundary are plotted in Fig. 2-5, which shows that a maximum of $\pm 28^\circ$ is required for the dynamic ϕ range.

In the above discussion we first showed that the location of main reflector illumination is very sensitive to ϕ scan, and then showed that a large ϕ-scan range is required to perform a circular scan coverage. These two points makes it necessary to tilt the feed to reduce the motion of the main reflector illuminated area.

The azimuthal feed tilt method can be explained using Fig. 2-6. Since the antenna system was synthesized according to a parent reflector system that is axisymmetric about z axis, the azimuthal feed tilt about z axis, given by angle ϕ_f, is equivalent to rotating the whole antenna about z axis by angle ϕ_f. Therefore, (2-8) becomes

$$\tan(\phi'_c - \phi_f) = \frac{(\cos\theta+1)\dfrac{\sin 2(\phi-\phi_f)}{2} \sin\theta_c - \sin\theta \sin(\phi-\phi_f) \cos\theta_c}{(\cos\theta \cos^2(\phi-\phi_f) - \sin^2(\phi-\phi_f)) \sin\theta_c - \sin\theta \cos(\phi-\phi_f) \cos\theta_c} \tag{2-12}$$

The values of ϕ'_c as functions of ϕ in (2-12) with various feed tilt angle ϕ_f are plotted in Fig. 2-3. The intersections between constant ϕ_f curves and the horizontal axis of Fig. 2-3 correspond to conditions for ϕ'_c=0 (no azimuthal motion for the main reflector illuminated area). While the antenna is scanning, (2-12) can be solved in real time for the ϕ'_c=0 condition to obtain the correct feed tilt angle ϕ_f for each ϕ-scan angle.

2.3. Choosing Mirror Motion Axes to Reduce the Mirror Size

The mirror is the major moving part in the reflector system; therefore, minimizing the size of the mirror is very important. The size of the mirror is determined by the illuminated area in the plane of the mirror and the relative motion between this illuminated area and the mirror. The mirror must cover the directly illuminated area (in GO sense) in the plane of the mirror at all scan angles. Moreover, the mirror must be oversized in order to reduce diffraction loss. In order to reduce the size of the mirror, the relative motion between the mirror and its illuminated area must be minimized; i.e. the mirror motion must follow the motion of the illuminated area in the mirror plane during scan.

The mirror motion during scan can be achieved by one degree of linear translation and rotation about two axis; see Fig. 2-6. In theory, there are several possible directions of the translational axis t as well as possible locations of the rotational axes y'_m and z'_m. Once all the axes are chosen, the amount of translation and rotation is determined from scan angles by a coordinate transformation from antenna coordinates to mirror coordinates. In order to reduce the relative motion between the mirror and its illuminated area, the t axis is best chosen to be along the ray from the subreflector illumination center to the virtual main reflector illumination center at zero ϕ-scan angle (this is the principal, or center, ray).

The z'_m axis can be chosen on the surface of the mirror. This, however, introduces relative motion between the mirror and its illuminated area during ϕ scan because of the feed azimuth tilt. To alleviate this problem, the rotational axis z'_m is chosen to be above the plane of the mirror; see Fig. 2-6. Since the rotational axis is off the mirror, the mirror translates during the rotation to follow the motion of illuminated area.

The choices for z'_m axis can be performed numerically by analyzing the coordinate data for the illumination center on the mirror at different scan angles. The graphical display of such data shows that the mirror area can be reduce by 50% by properly choosing z'_m axis.

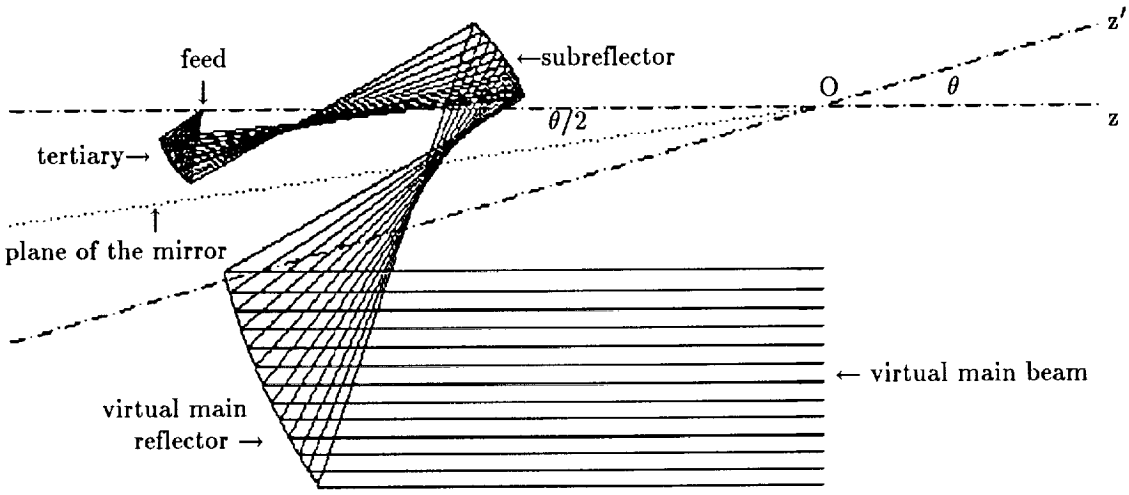

a. Basic spherical tri-reflector system.

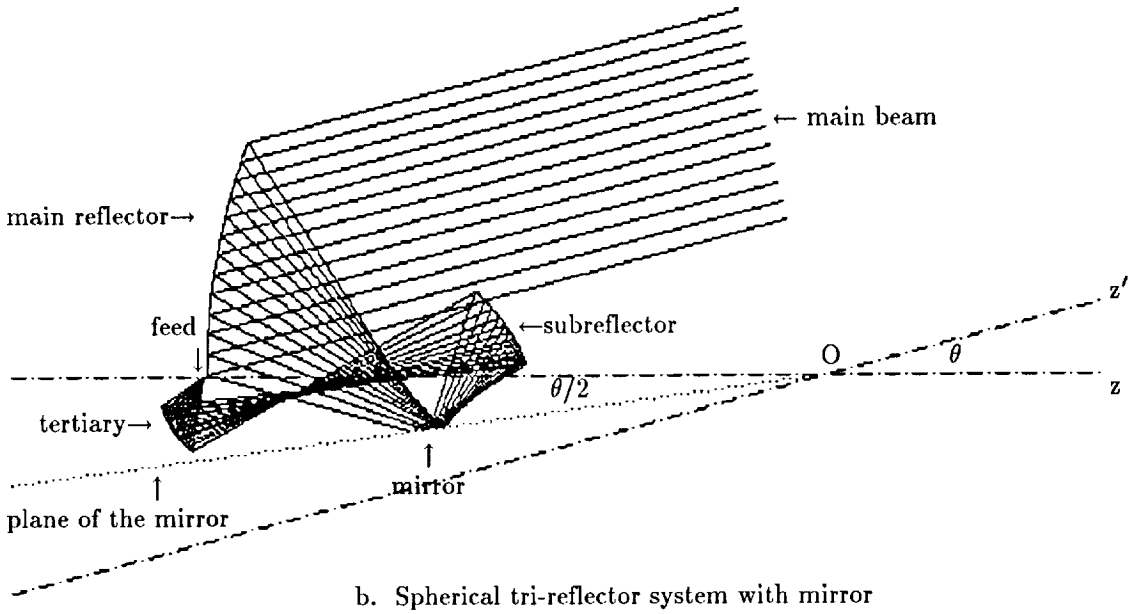

b. Spherical tri-reflector system with mirror

Figure 2-1. The scanning function of the mirror in a spherical tri-reflector system

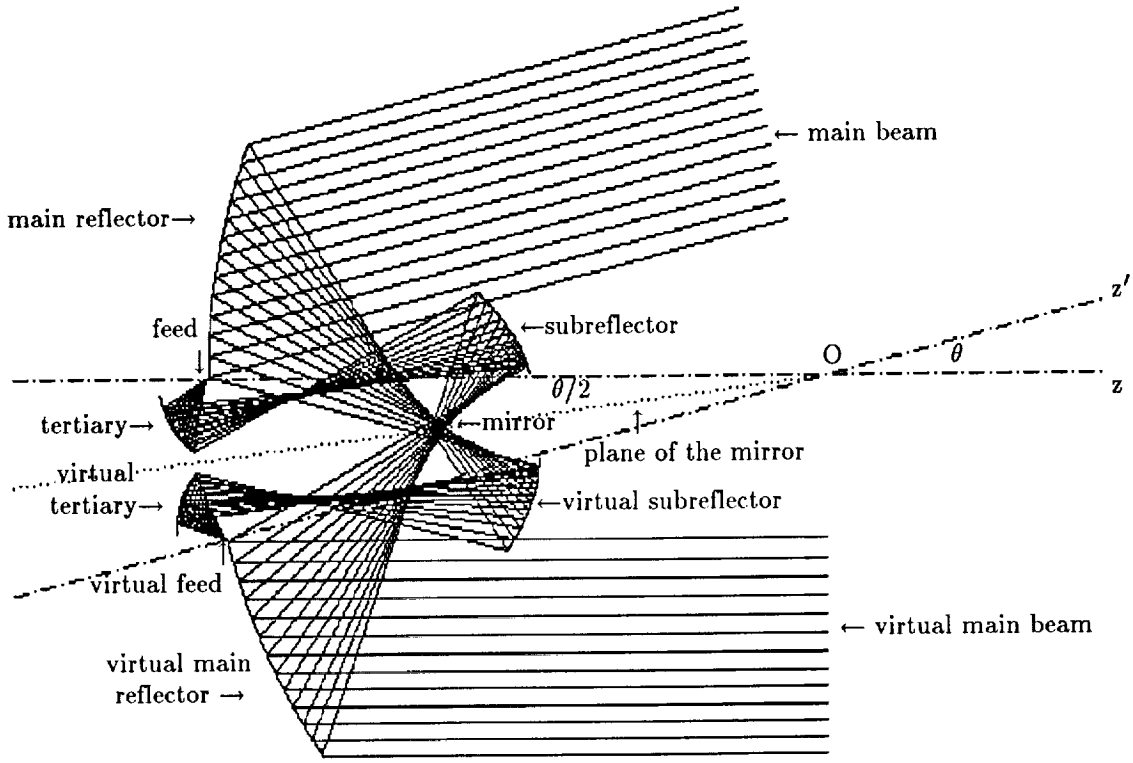

c. Illustration for mirror imaging scanning process

Figure 2-1. (continued)

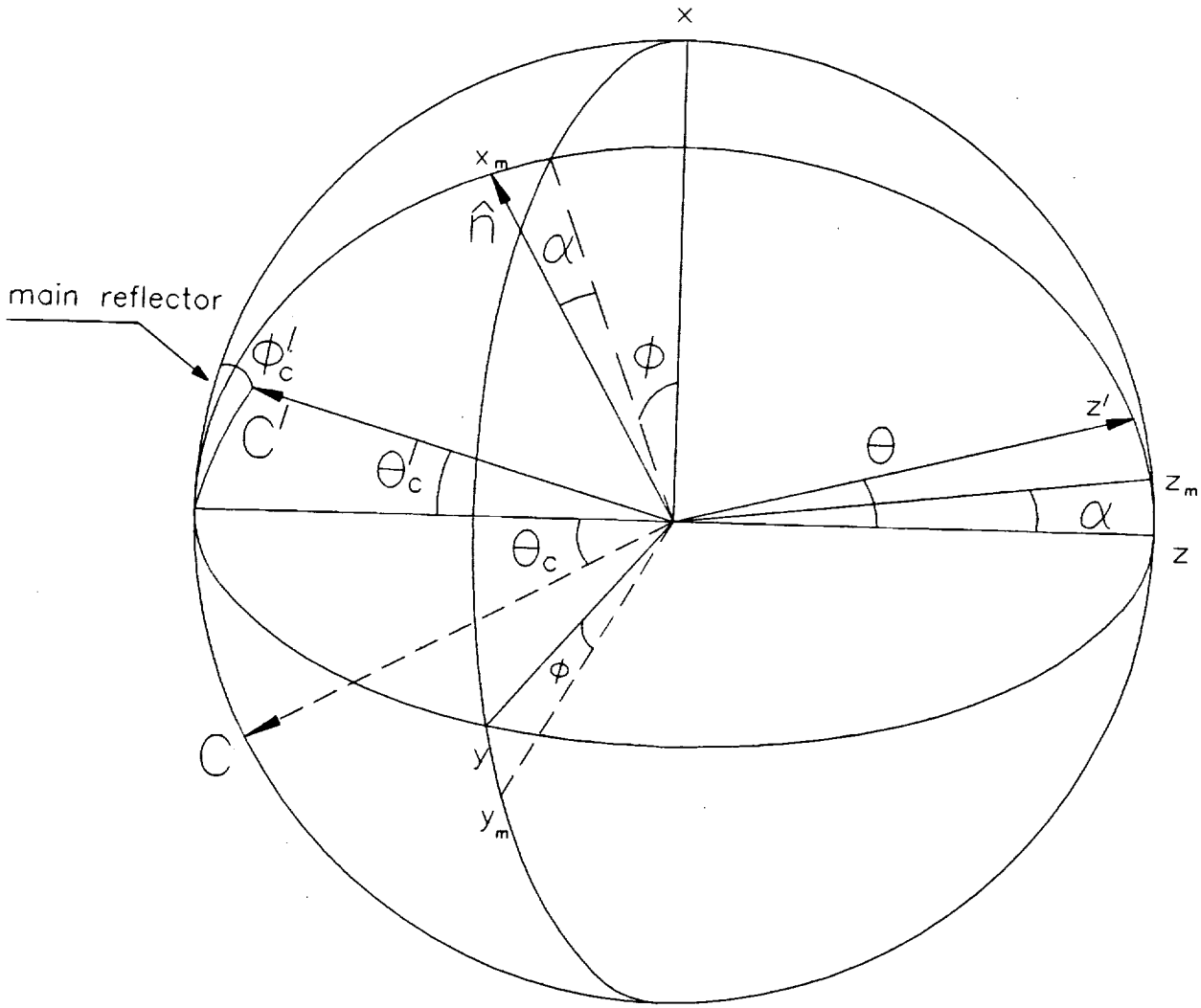

Figure 2-2. Geometry for mirror coordinates and antenna coordinates.

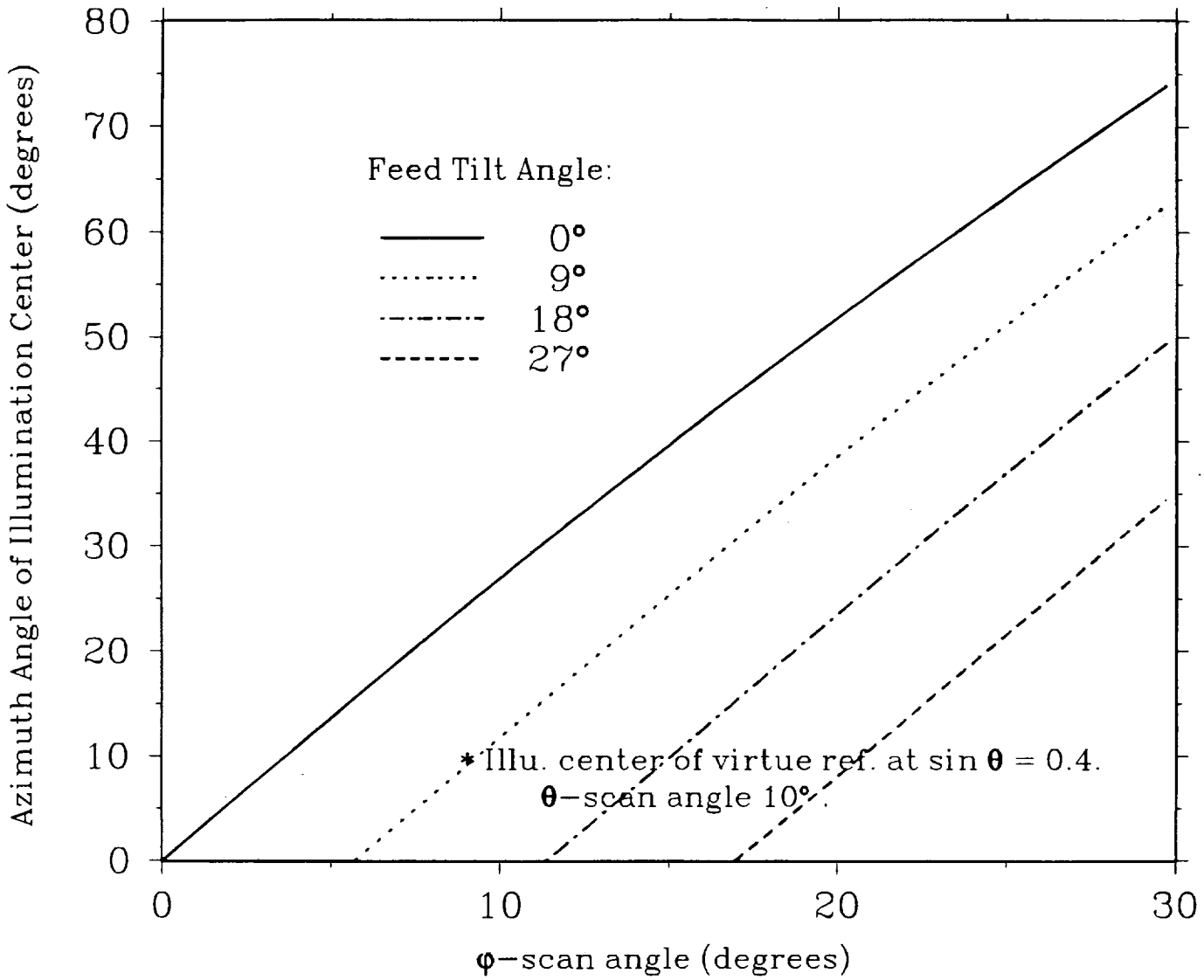

Figure 2-3. Motion of illumination center with ϕ scan for various feed tilt angles.

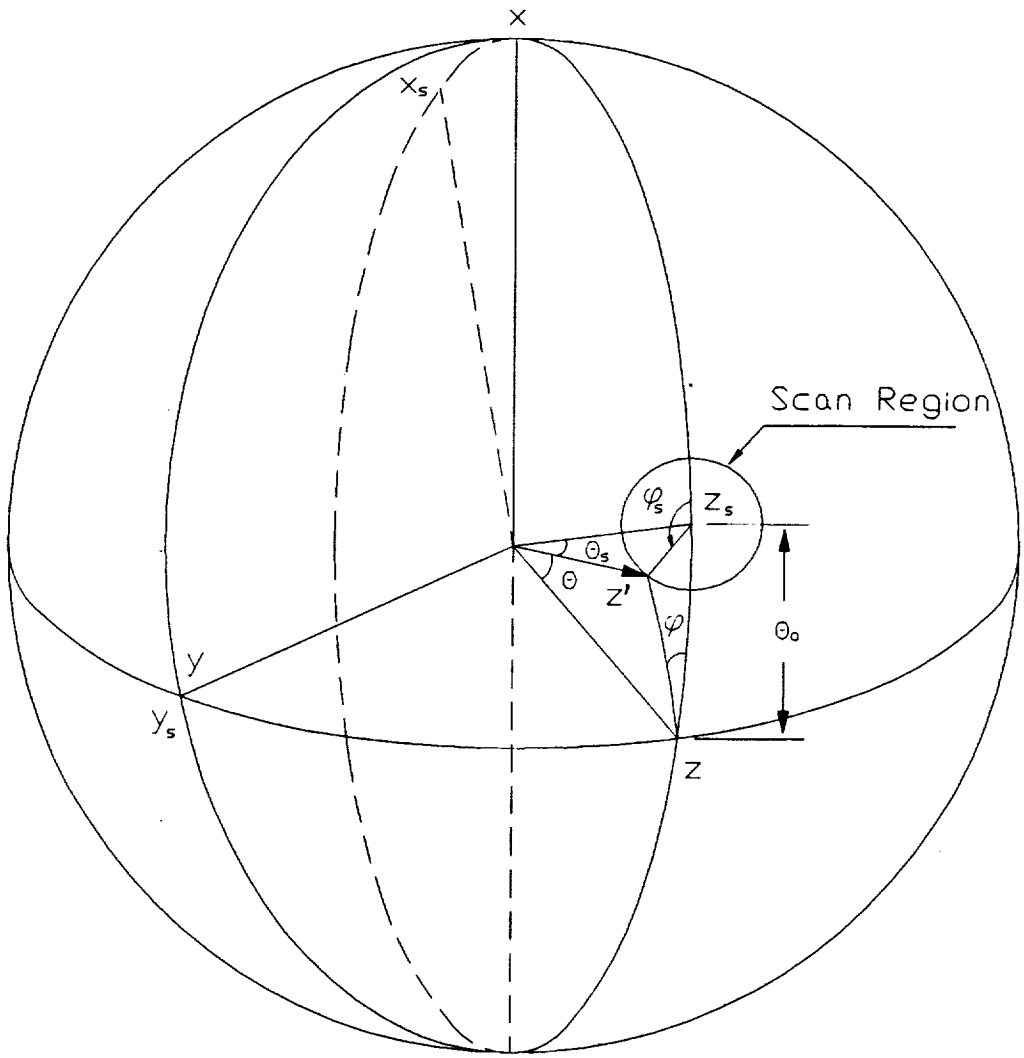

Figure 2-4. Geometry for scan coordinates and antenna coordinates.

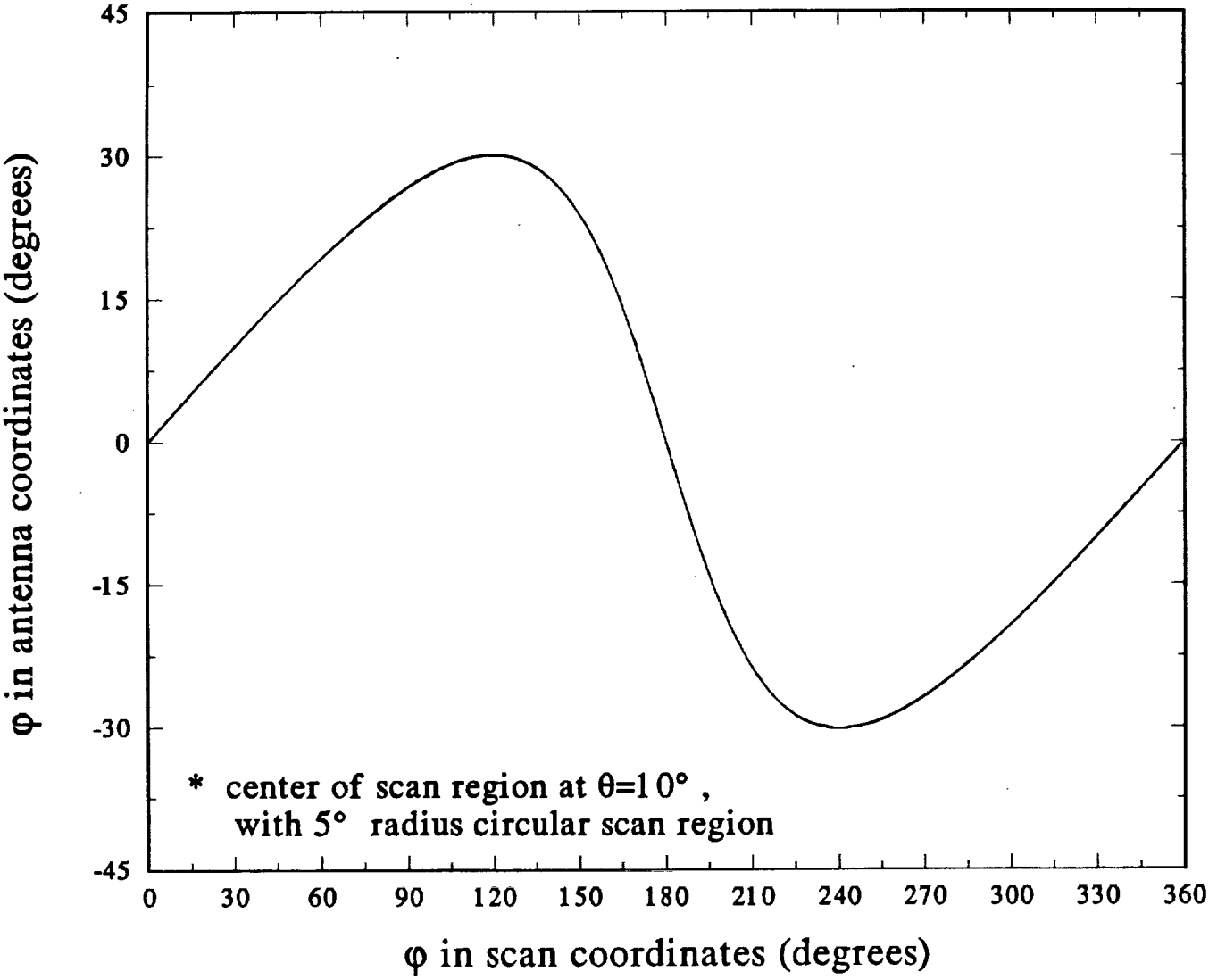

Figure 2-5. Dynamic range of antenna ϕ coordinate.

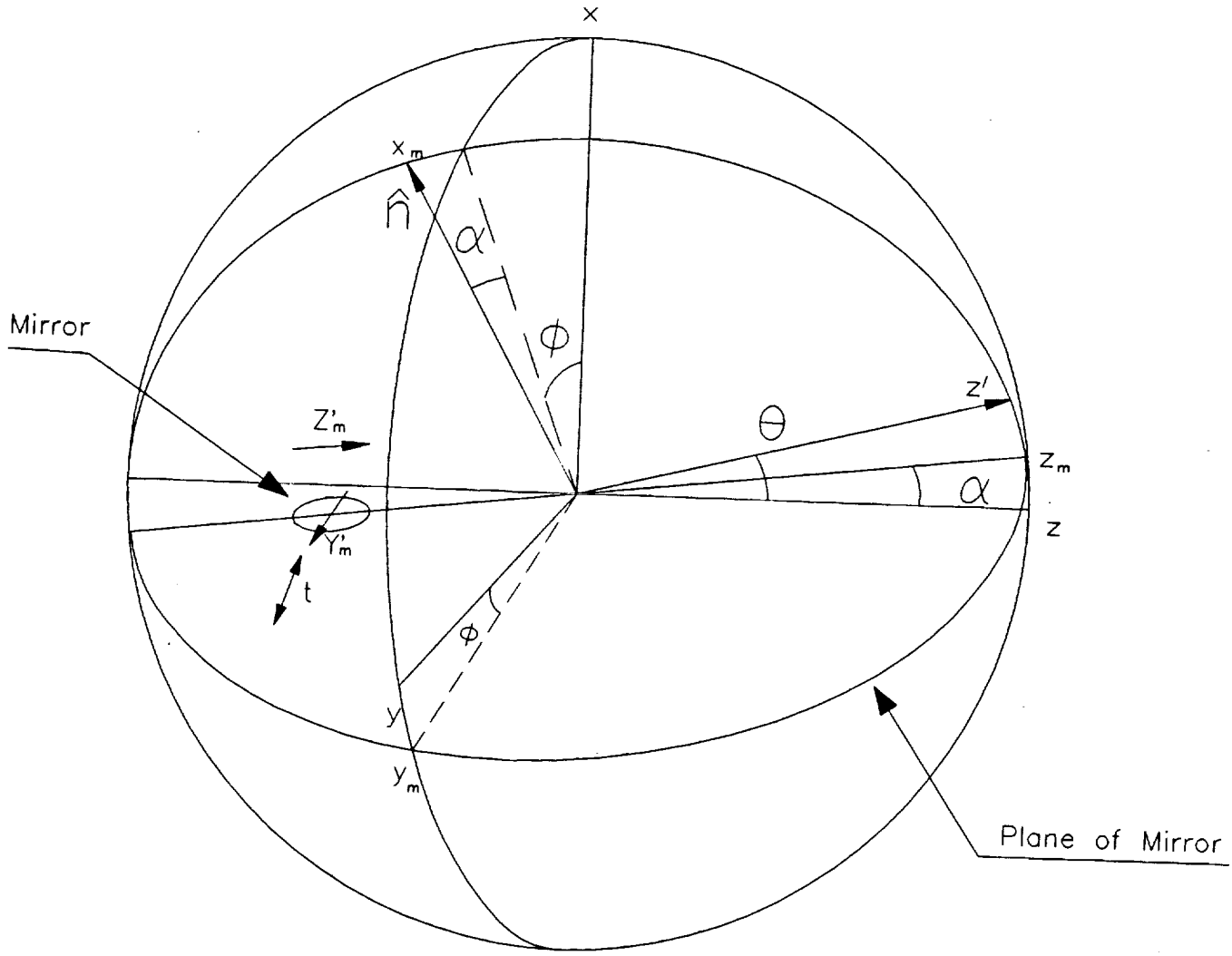

Figure 2-6. Geometry for mirror translation and rotation axes.

Chapter 3
OPTIMIZATION OF REFLECTOR CONFIGURATIONS

3.1. Introduction

The majority of existing reflector antennas are single focal point antenna systems with a pair of imaging points: one at the focal point and the other at infinity. A common property shared by the single focal point antennas is their ability to transform a spherically spreading wave originated from the focal point to a plane wave propagating outward along the axis of reflector. Limited scanning of main beam using single focal point reflector antennas can be accomplished by displacement of feed antenna from the focal point which introduces the necessary phase tilt in the aperture field distribution. Alternatively, beam scanning can be accomplished by the displacement of subreflectors in multiple reflector systems. The displacement of the subreflector simulates the displacement of feed image. Both Type 1 and Type 2 configurations developed at VA Tech are single focal point reflector systems where the main beam is scanned by the displacement of secondary and tertiary reflectors, respectively.

The EM performance of single focal point reflector antennas degrades as the main beam is scanned off-axis. The performance of a reflector antenna can be evaluated most easily by the gain of the radiation pattern. When gain is reduced both main beam beamwidth and sidelobe levels increase by the amount equal to the loss in gain. The gain is affected primarily by three causes:

1. Aperture phase distribution
2. Aperture amplitude distribution
3. Feed spillover

In the synthesis of high gain reflector antennas the aperture phase error has the most effect to the gain. Thus, the uniform phase distribution over the aperture plane is satisfied first during the synthesis. The specified aperture amplitude distribution and feed spillover are often only approximately satisfied.

In the wide scan angle reflector antennas all three causes have similar magnitude of effects to the radiation pattern. When reflector antennas are synthesized based on the aperture phase error, such as the single focal point reflector systems, the scan capability of the antennas are sometimes limited by the other causes. For example, a detailed analysis of the VA Tech Type 1 system shows that the scan range is limited by the feed spillover. [1]

The scan performance of reflector antennas can be improved by optimizing the displacement of feed or subreflectors and by optimizing the reflector surface shape. The

optimization is performed such that all three causes that degrade the radiation pattern are minimized simultaneously within the specified limits of scan. The optimization procedure requires an initial reflector configuration. When a single focal point reflector configuration is specified as the initial geometry, then the optimization procedure increases the aperture phase error while reducing the feed spillover and the aperture amplitude distribution. As a result the radiation pattern degrades slightly for the unscanned beam while the radiation pattern improves at the limits of the scan.

3.2. Error Functional Definition

The optimization of scan capability of reflector antenna systems is accomplished using code GROP. GROP is a collection of modules consisting of the routines to define the reflector configurations, the routines for Geometrical Optics based analysis in both transmit and receive modes, and the routines for optimization of a reflector configuration for wide angle scan. Depending on the configuration of reflector systems and type of optimization applied for wide angle scanning, different routines are linked to form a computer program. In this report the results of scan optimization for the Type 1 system accomplished by the program DROP (Dual Reflector Optimization Program) is discussed. The improved Type 1 system will be noted as Type 1A system.

The analysis of the Type 1 system shows that the scan range of the system is limited by the feed spillover. [1] Thus, it is important to emphasize the minimization of the spillover error to improve the scan capability of Type 1 configurations. In the Type 1A system the translation and rotation of secondary reflector is confined about a center point $\vec{P}_{20}$ of illuminated region on the secondary reflector along the principal ray as shown in Fig. 3.2-1. The principal ray is defined as a line between the center of projected aperture of the primary reflector and the virtual focal point the primary reflector for a given scan angle. The virtual focal point is determined using receive mode GO ray tracing. The rays are traced from the aperture plane tilted to a specified scan direction to the primary reflector surface which are reflected from the surface to form a caustic region. Suppose a position on i-th ray for a given path length from the aperture plane is represented by $\vec{r}_i$. The virtual focal point is determined by the point $\vec{r}_{VF}$ such that the variance

$$v = \sum_{i=1}^{N} \frac{1}{N}\left(\vec{r}_i \quad \vec{r}_{VF}\right) \tag{3-1}$$

is minimum. Confining the secondary reflector translation to be along the principal ray increases the feed spillover efficiency since the majority of plane wave energy incident on

the primary reflector that is reflected towards the virtual focal point is captured by the secondary reflector.

The center of illuminated region point, $\vec{P}_{20}$, on the secondary reflector is fixed to the physical center of secondary reflector aperture when the secondary reflector rim is determined by the GO edge rays on the primary reflector for the unscanned beam. When the diameter of secondary reflector is enlarged, then the point $\vec{P}_{20}$ can be allowed to float for a given scan angle. It is then possible to determine $\vec{P}_{20}$ to minimize overall displacement of the secondary reflector. For example, when the beam is scanned to $+\theta$ direction in $\phi = 0^{\circ}$ plane the principal ray would move down towards the -x axis. Thus, $\vec{P}_{20}$ can be moved towards -x on the secondary reflector surface to compensate for the displacement of principal ray for the scanned beam.

The Type 1A antenna system used for synthesis consisted of an offset paraboloidal primary reflector with 10.63 meter projected aperture diameter and 7.795 meter offset height and a hyperboloidal secondary reflector which are equivalent to the Type 1 configurations as shown in Fig. 3.2-2. [1] The subreflector diameter was increased from 1.5 meters to 2.2 meters. The required translational and rotational displacement of the secondary reflector as a function of elevation angle θ for scanning in 0°, 45°, 90°, 135° and 180° in ϕ plane are shown in Figs. 3.2-3 through 3.2-8. The definition of α and β rotations are the same as Type 1 system. [1] Since the system is symmetric with respect to the xz-plane, the required displacement for ϕ angles from 180° to 360° are the same for x and z translation and α rotation, but the negative of y translation and β rotation. Comparison of required translation and rotation at $\theta = 1^{\circ}$ scan for the Type 1 and Type 1A systems are given in Table 3-1. It is apparent that there is considerable reduction in required subreflector displacement achieved by increase in diameter of the secondary reflector. In fact, it may be possible to achieve a similar scan performance without any translational displacement of secondary reflector.

3.3. Electromagnetic Analysis Results

Electromagnetic analysis of Type 1A reflector antenna system was performed at 18 GHz using GRASP7 reflector analysis package. GO/GTD analysis was used at the secondary reflector followed by PO analysis on the primary reflector. The system was fed by a feed fixed at the unscanned feed point and pointed correctly for the unscanned beam. The feed taper was chosen to be 15 dB at 0.75 meter from the center of illuminated region of the secondary reflector for the unscanned beam.

Figure 3.3-1 shows the main beam peak gain of the antenna system as a function of scan angle for the Type 1A system. The scan range of approximately 1.4° calculated

Table 3-1

Comparison of required translational and rotational displacements of the secondary reflector, and the gain loss from the unscanned gain maximum at an operating frequency of 18 GHz.

(a) Type 1 configuration

ϕ (deg)	T_X (m)	T_Y (m)	T_Z (m)	T_{Total} (m)	α (deg)	β (deg)	ΔG (dB)
0	0.327	0.000	0.182	0.374	-8.47	0.00	-3.88
45	0.143	0.256	0.078	0.304	-4.58	6.02	-2.81
90	-0.096	0.174	-0.053	0.205	1.33	6.09	-1.79
135	-0.125	0.038	-0.074	0.150	4.35	3.34	-1.61
180	-0.103	0.000	-0.066	0.122	5.18	0.00	-1.58

(b) Type 1A configuration

ϕ (deg)	T_X (m)	T_Y (m)	T_Z (m)	T_{Total} (m)	α (deg)	β (deg)	ΔG (dB)
0	-0.002	0.000	0.004	0.005	-4.00	0.00	-0.47
45	-0.004	0.003	0.001	0.005	-2.74	3.15	-0.43
90	0.007	0.000	0.002	0.007	0.00	4.31	-0.39
135	-0.011	0.009	0.001	0.014	2.67	3.08	-0.37
180	-0.001	0.000	-0.003	0.004	3.86	0.00	-0.32

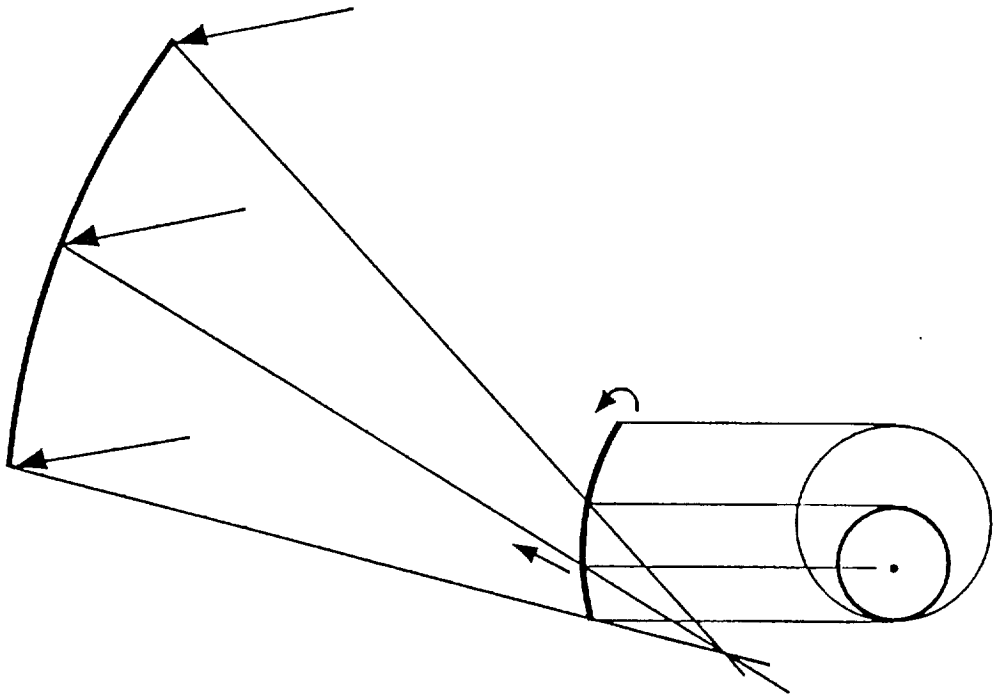

Figure 3.2-1. Secondary reflector displacement optimization procedure for Type 1A configuration.

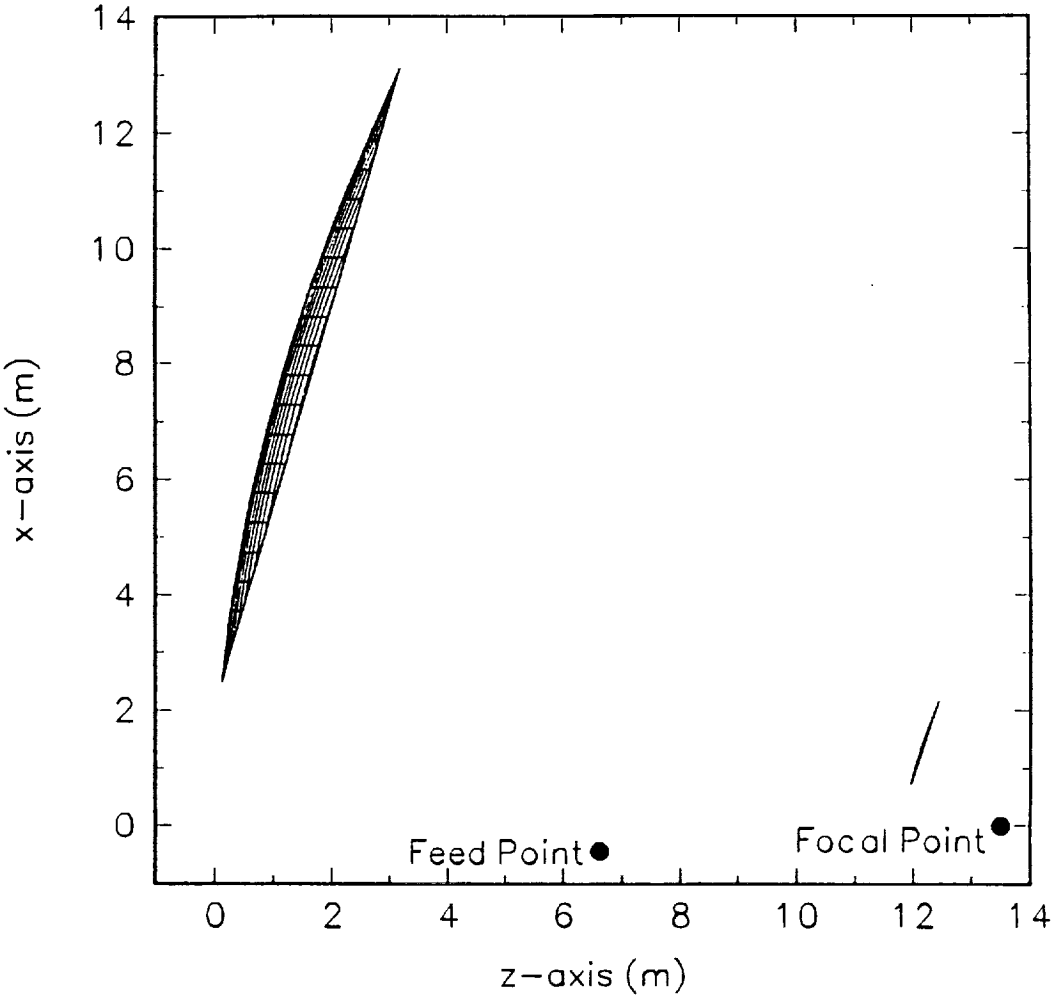

Figure 3.2-2. Type 1 and Type 1A reflector antenna system configuration. (profile)

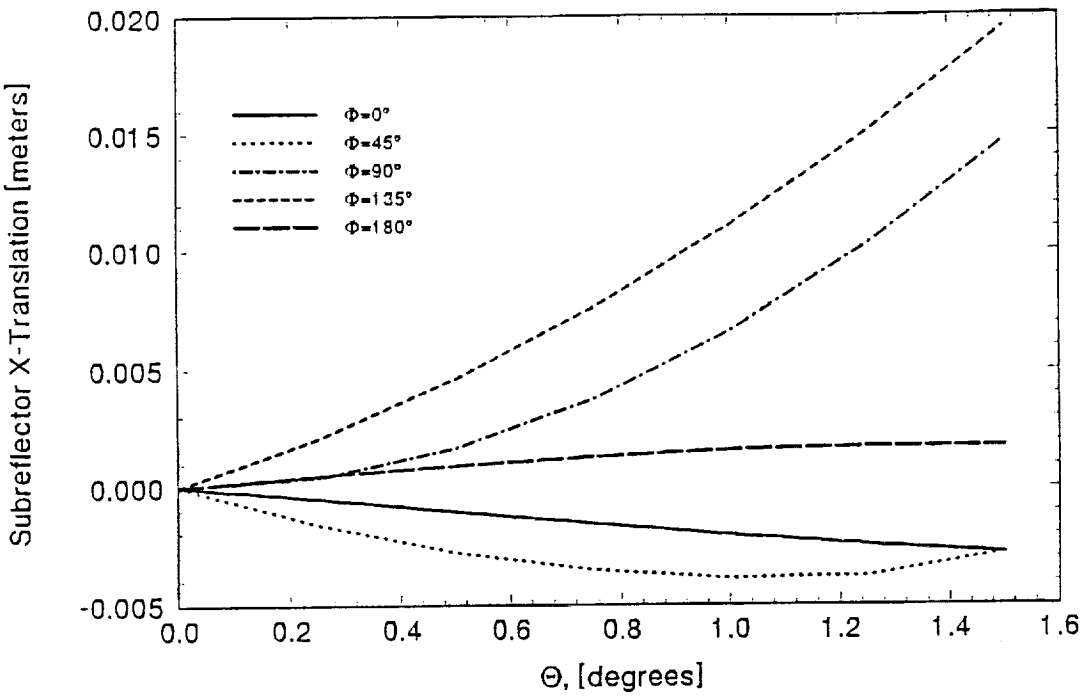

Figure 3.2–3 Secondary reflector translation in the x-direction for Type 1A reflector antenna system.

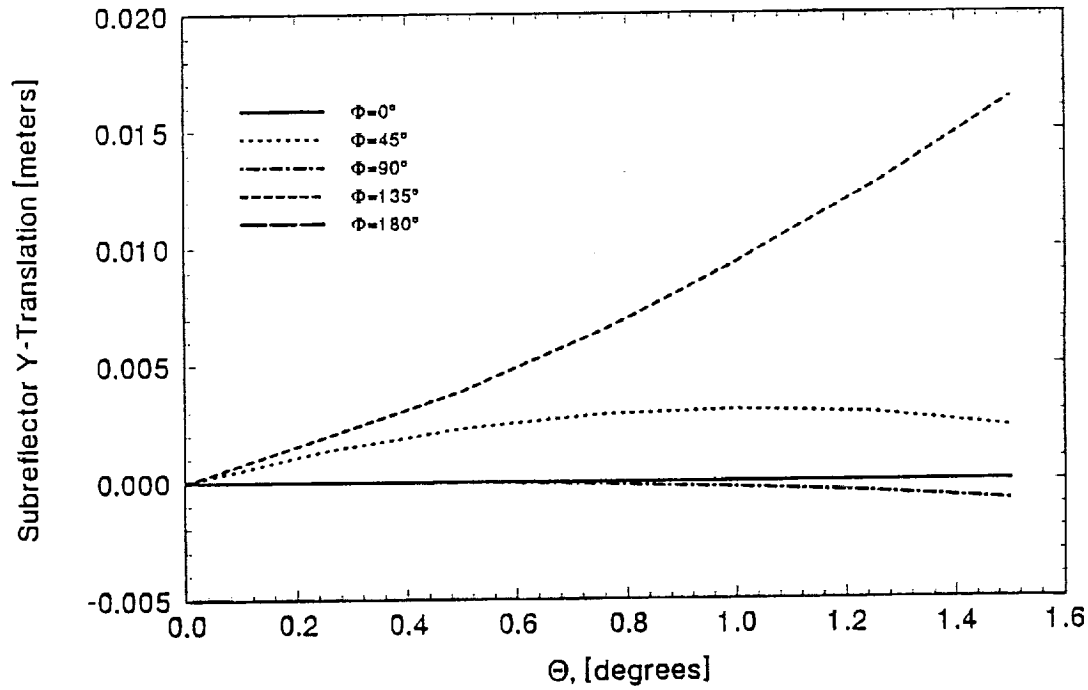

Figure 3.2–4 Secondary reflector translation in the y-direction for Type 1A reflector antenna system.

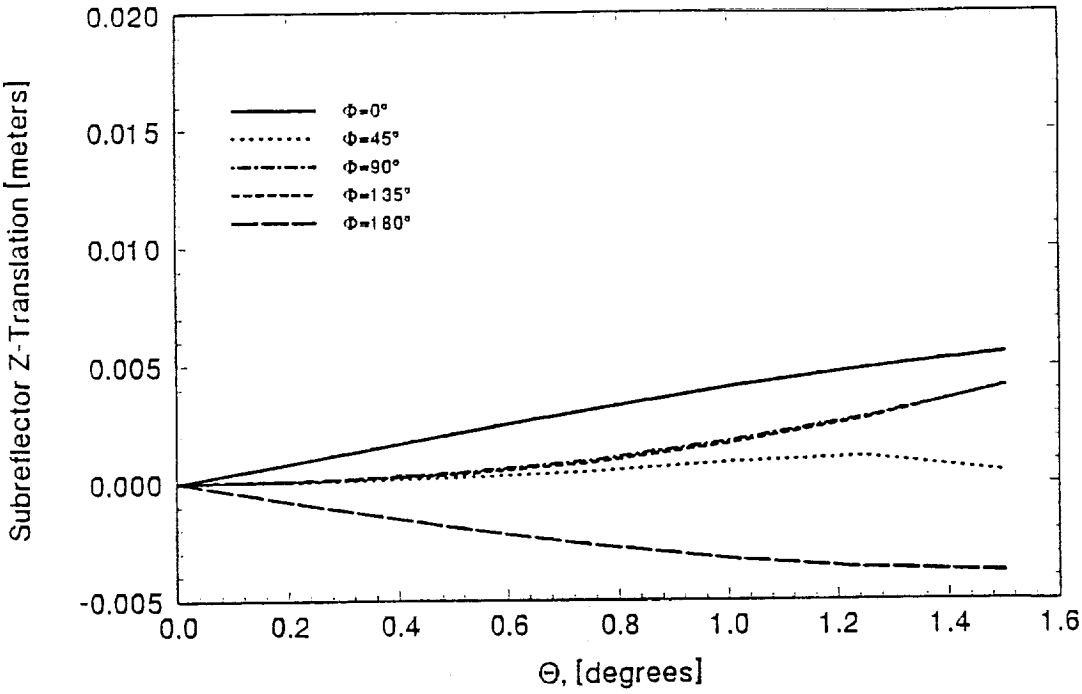

Figure 3.2–5 Secondary reflector translation in the z-direction for Type 1A reflector antenna system.

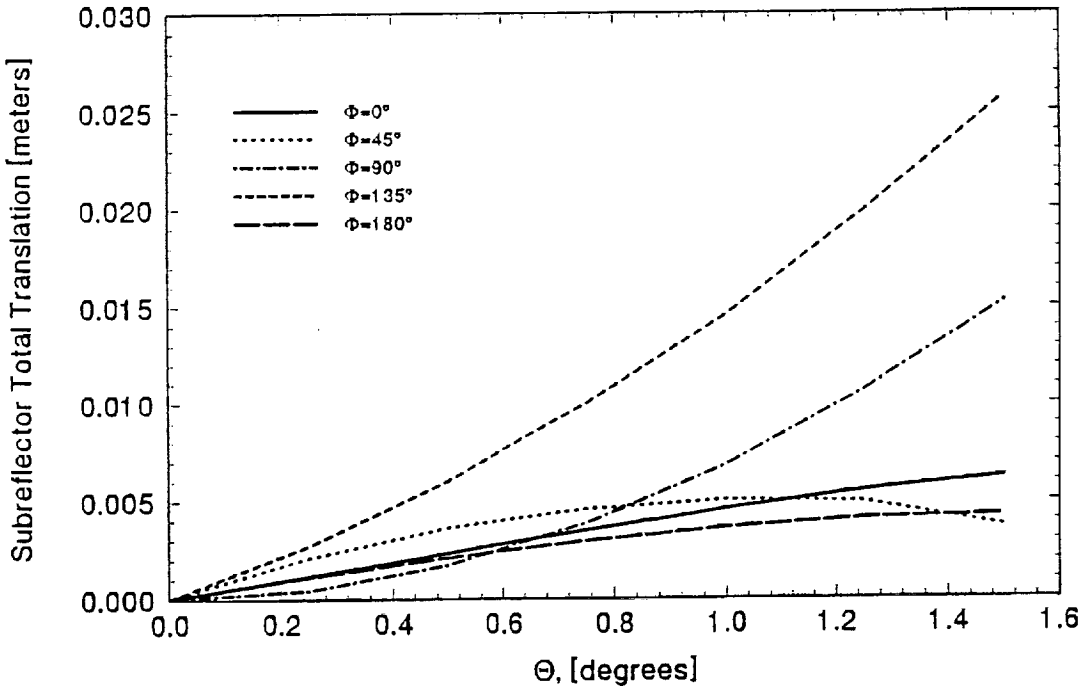

Figure 3.2–6 The total linear secondary reflector translation for Type 1A reflector antenna system.

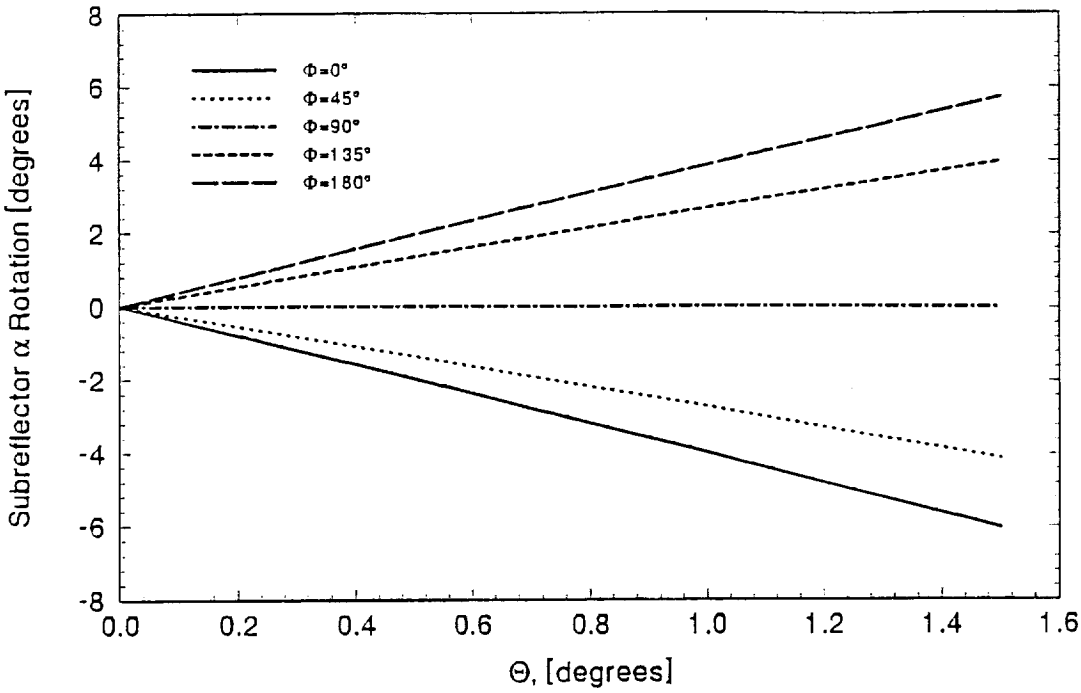

Figure 3.2–7 Secondary reflector α rotation for Type 1A reflector antenna system.

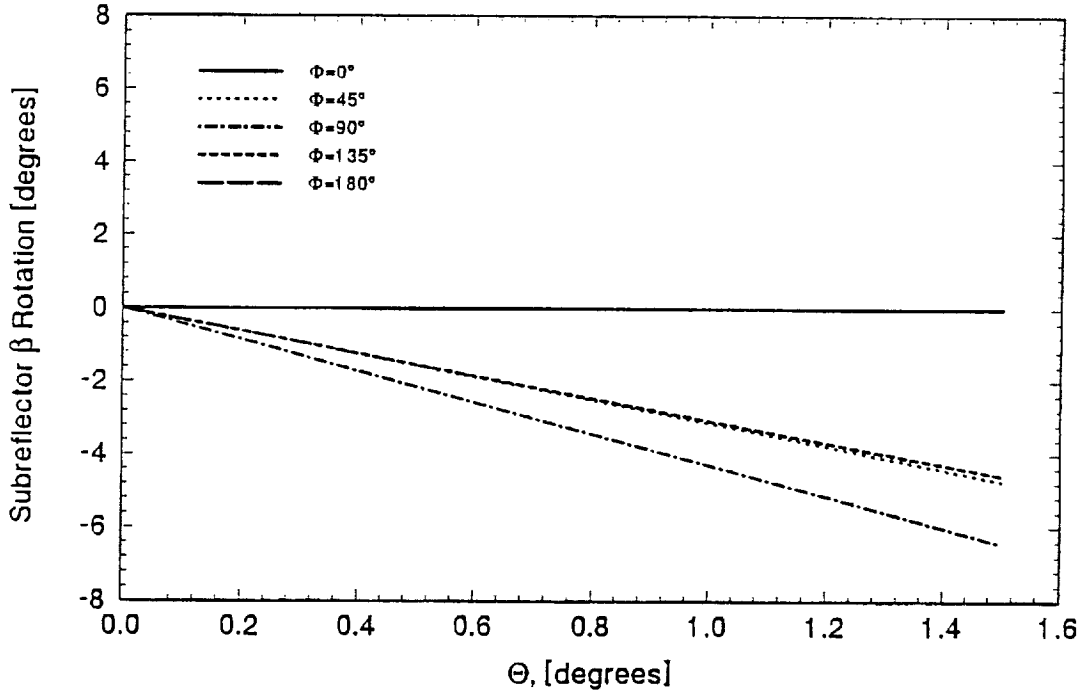

Figure 3.2–8 Secondary reflector β rotation for Type 1A reflector antenna system.

using a 1 dB gain loss criteria is achieved. This is more than twice the scan range achieved by Type 1 system which has the maximum scan range of approximately 0.6°. [1] Unlike the Type 1 configuration, the scan range of the Type 1A system is not limited by spillover loss, which is apparent from Fig. 3.2-2. However, the increase in the scan range cannot be achieved at the higher frequency of operation because the aperture phase error becomes dominant cause for the gain loss.

3.4. Future Work

Future work on the optimization of reflector configurations for wide scanning include the following:

(1) Dual reflector scanning by the rotational displacement of an oversized secondary reflector with no translational displacement.

(2) Secondary reflector positioning error sensitivity study on Type 1A system.

(3) Comparison of scan capability between Type 1 and Type 1A configurations for operation at higher frequency.

(4) Application of optimization on Type 2 system.

3.5. References

1. W.L. Stutzman, et al., *Feasibility Study of a Synthesis Procedure for Array Feeds to Improve Radiation Performance of Large Distorted Reflector Antennas*, Semiannual Status Report, September 1992.

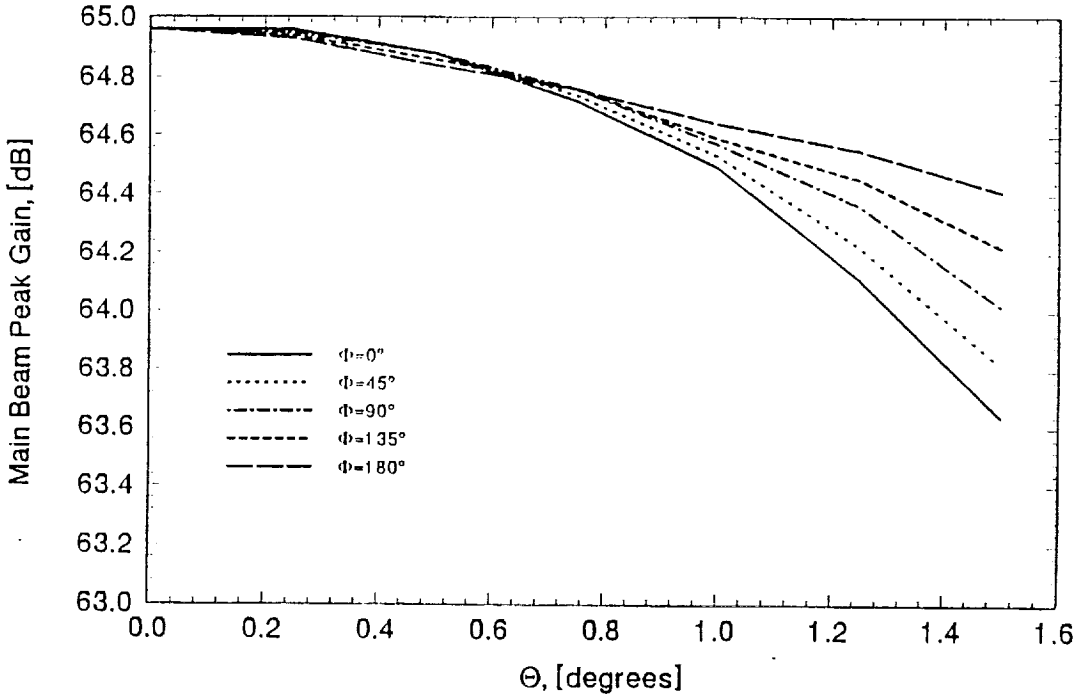

Figure 3.3–1 Main beam gain as a function of scan angle for Type 1A reflector antenna system.

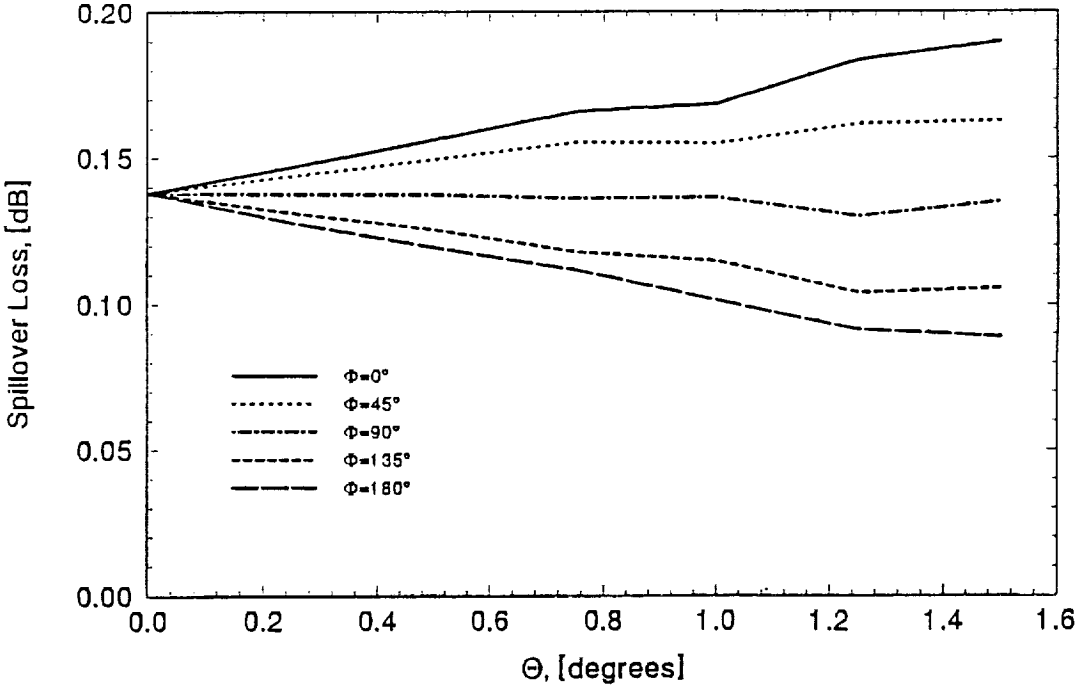

Figure 3.3–2 Feed spillover efficiency as a function of scan angle for Type 1A reflector system.

Chapter 4
PUBLICATIONS

4.1. Recent Publications

4.1.1. Conferences

(1) P.C. Werntz, K. Takamizawa, W.L. Stutzman and P. Foldes, "Wide Scanning Tri-Reflector System with an Elliptic Subreflector and Moving Tertiary Reflector," URSI Radio Science Meeting (Boulder, CO), January 1992.

(2) R.M. Barts, W.A. Davis and W.L. Stutzman, "A Multiport Noise Model with Applications to Remote Sensing Arrays," URSI Radio Science Meeting (Boulder, CO), January 1992.

(4) P.C. Werntz, M.C. Bailey, K. Takamizawa and W.L. Stutzman, "Array-Fed Reflector Antenna Systems for Wide Scan," AP-S Symposium, July 1992.

(5) K. Takamizawa, P. Werntz, and W.L. Stutzman, "Optimization of Multiple Reflector Antenna Configuration for Wide Angle Scan," AP-S Symposium, July 1992.

(6) J. LaPean and W.L. Stutzman, "Beam Scanning in the Cassegrain Antenna System by the use of Subreflector Movement," AP-S Symposium, July 1992.

(7) B. Shen and W.L. Stutzman, "Beam Efficiency Evaluation of Large Reflector Radiometer Antennas," URSI Meeting, Jan. 1993.

(8) B. Shen and W.L. Stutzman, "Methods to Improve the Aperture Efficiency and Simplify the Mechanical Motion of Spherical Main Reflector Scanning Antennas," URSI Meeting, Jan. 1993.

5.1.2. Papers

(1) W.T. Smith and W.L. Stutzman, "A Pattern Synthesis Technique for Array Feeds to Improve Radiation Performance of Large Distorted Reflector Antennas," IEEE Trans. on Ant. and Prop., Vol. 40, pp. 57-62, January 1992.

5.2. Planned Publications

5.2.1. Conferences

5.2.2. Papers

(1) B. Shen and W.L. Stutzman, "Design of Scanning Tri-Reflector Antennas with High Aperture Efficiency," to appear in IEEE Trans. Ant. and Prop..

(2) P. Werntz and W.L. Stutzman, "Wide Scanning Tri-Reflector Antenna System Using Moving Tertiary Reflector," submitted to IEEE Trans. on Ant. and Prop..

(3) J.W. LaPean and W.L. Stutzman, "Wide Scanning Dual Reflector Antennas Using a Moving Subreflector," to be submitted.

(4) K. Takamizawa and W.L. Stutzman, "Optimization of Multiple Reflector Antenna Performance Under Parameter Constraints," IEEE Trans. on Ant. and Prop., to be submitted.

(5) B. Shen and W.L. Stutzman, "Design of a Scanning Spherical Tri-Reflector Antenna with a Mirror," to be submitted.

(6) B. Shen and W.L. Stutzman, "Antenna Design for Optimum Radiometric Temperature Resolution," to be submitted.

(7) R.M. Barts and W.L. Stutzman, "Noise Modeling of Array Antennas with Applications to Microwave Remote Sensing," IEEE AP-S Trans., to be submitted.

5.2.3. Theses, dissertations, reports

(1) P.C. Werntz, "Novel High Gain Wide Scan Tri-Reflector Antennas," Ph.D. dissertation, 1993.

(2) J.W. LaPean, "Beam Scanning in the Cassegrain Antenna System Using a Moving Subreflector," Master's Thesis, Virginia Tech, 1993.

(3) K. Takamizawa, "Optimization of Multiple Reflector Antenna Performance Under Parameter Constraints," Ph.D. dissertation, Virginia Tech, 1993.

(4) B. Shen, "Design of High Efficiency Spherical Reflector Antennas with Multiple Subreflector for Wide Scan," Ph.D. dissertation, August 1993.

(5) R.M. Barts, "Applications of Array Antennas to Microwave Remote Sensing," Ph.D. dissertation, August 1993.

Distribution

1. NASA Langley
   M.C. Bailey
   T.G. Campbell
   L.C. Schroeder
2. NASA (3 copies)
   NASA Center for Aerospace Information
   P.O. Box 8757
   Baltimore/Washington International Airport, MD 21240
3. Peter Foldes, Inc.
4. VPI & SU Sponsored Programs (cover sheet)